KeAi

CHINESE ROOTS
GLOBAL IMPACT

#### Contents lists available at ScienceDirect

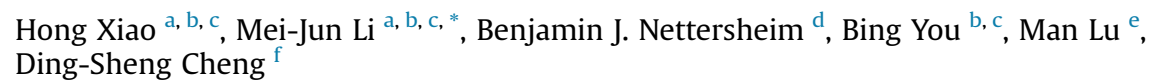
# Petroleum Science

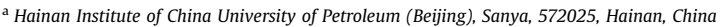
journal homepage: www.keaipublishing.com/en/journals/petroleum-science



# Original Paper

# Late Cretaceous marine incursion into central Africa





- <sup>b</sup> State Key Laboratory of Petroleum Resources and Engineering, China University of Petroleum (Beijing), Beijing, 102249, China
- <sup>c</sup> College of Geosciences, China University of Petroleum (Beijing), Beijing, 102249, China
- <sup>d</sup> MARUM Center for Marine Environmental Sciences and Faculty of Geosciences, University of Bremen, 28359, Bremen, Germany
- <sup>e</sup> Molecular Eco-Geochemistry Laboratory, Department of Geological Sciences, University of Alabama, Tuscaloosa, AL 35485, USA
- f Research Institute of Petroleum Exploration and Development, PetroChina, Beijing, 100083, China



## ARTICLE INFO

Article history: Received 19 August 2024 Received in revised form 14 November 2024 Accepted 26 February 2025 Available online 27 February 2025

Edited by Jie Hao

Keywords: Late Cretaceous transgression Molecular fossils Dinosteranes Neotethys ocean Central Africa

#### ABSTRACT

The Late Cretaceous global transgression is one of the best documented episodes of continental submergence events. The extent of transgression of the Neotethys Ocean into the African continent is generally thought to be limited to north Africa. Here, we describe transgression traces in the Muglad Basin in central Africa that indicate a greater spatial extend of the Neotethys during the late Cretaceous. A series of molecular markers detected in the Upper Cretaceous Santonian-Maastrichtian sediments of the Muglad Basin are typical for marine depositional conditions and differ from those in the typical lacustrine sediments of the Lower Cretaceous Barremian-Aptian. Combining the geological-geochemical implications of these markers with the paleogeographic, paleontological and lithological records, we propose that the Muglad Basin received intermittent marine inundations during the Santonian-Maastrichtian stages (86.3—66.0 Ma) and these special molecular markers are therefore the products of seawater incursion. Consequently, this study proposes that the transgression extent of the Neotethys Ocean into the African continent southern extended to the central Africa during the Late Cretaceous. © 2025 The Authors. Publishing services by Elsevier B.V. on behalf of KeAi Communications Co. Ltd. This is an open access article under the CC BY-NC-ND license (http://creativecommons.org/licenses/by-nc-nd/

# 1. Introduction

During the Late Cretaceous, the Gondwanaland province had split into its five constituents (Guiraud et al., 2005) and the sealevel remained at the highest level (Miller et al., 2005), resulting in a thalassocratic state of dispersed continents (Veevers, 2004). The high sea-level with warm climate not only leads to a large area of epicontinental sea environments and promoted phytoplankton evolution (Miller et al., 2005), but also widespread deposition of a set of organic-rich sediments as important source rocks in many petroliferous basins around the world (Hou et al., 2000; Guiraud et al., 2005; An et al., 2017). Therefore, the sea-level increase and extension of the Late Cretaceous global transgression have been the subject of geological interest for decades. Generally, as the stable northern margin of the Gondwanaland (Goncuoglu and Kozlu, 2000; Veevers, 2004; Badalini et al., 2006), the North African

continent should be very sensitive to the Late Cretaceous transgression events. Based on the systematic review and analysis of the stratigraphy and sedimentary data of more than 20 basins in north Africa, it was concluded that the Kufra Basin (Libya) located in the north of Muglad Basin (Sudan and South Sudan) is the extreme south of transgressed continental shelf during the Late Cretaceous (Fig. 1) (Lüning et al., 2000; An et al., 2017). Accordingly, the Muglad Basin has always been regarded as a Mesozoic-Cenozoic continental basin without any traces of marine sedimentary record in its geological history (Schull, 1988; Guiraud and Maurin, 1992), and the Lower Cretaceous Barremian-Aptian lacustrine organic-rich sediment (also namely Abu Gabra Formation) is widely recognized as the unique source rock in the basin (Makeen et al., 2015). Although the vast majority of discovered hydrocarbon resources in the Muglad Basin are generated from the Barremian-Aptian lacustrine source rocks, recently Xiao et al. (2019a) found that the individual Upper Cretaceous Santonian and Maastrichtian samples yield very different organic geochemical features compared to the lacustrine samples (Xiao et al., 2019a). This study firstly revealed a

E-mail address: meijunli@cup.edu.cn (M.-J. Li).

<sup>\*</sup> Corresponding author.

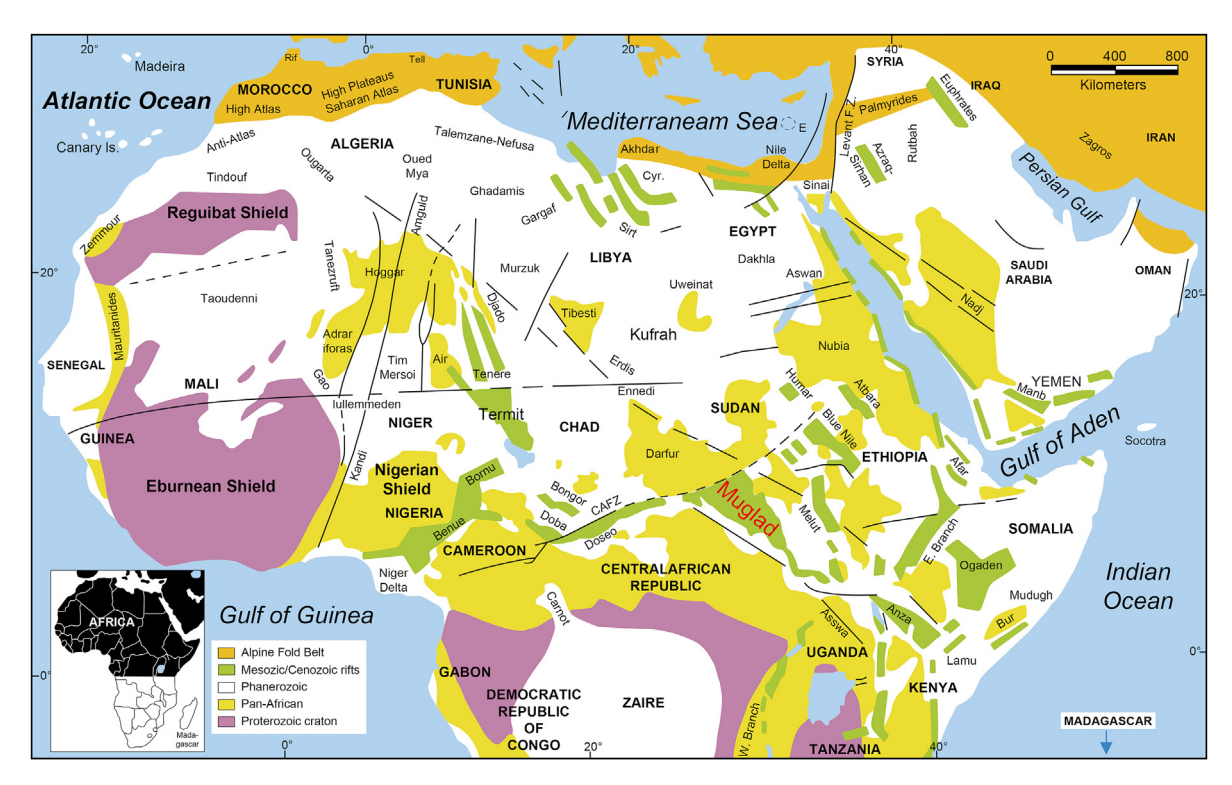


Fig. 1. Schematic geological map of North Africa, Central Africa and Arabia, and geographic location of Muglad Basin (Modified from Guiraud et al., 2005; An et al., 2017).

new type of potential hydrocarbon resource in the basin, but did not assess whether the basin was affected by seawater and/or marine transgressions.

Here we comprehensively analyze the molecular marker composition, paleogeographic and paleontological records in the Late Cretaceous Santonian-Maastrichtian and Early Cretaceous Barremian-Aptian stages. The authors propose that the Muglad Basin received intermittent marine inundations during the Santonian-Maastrichtian rifting episode (86.3—66.0 Ma), then resulting in the various marine signatures observed in the Santonian-Maastrichtian sediments. Moreover, this study provides strong evidences for seawater incursion into Muglad Basin, and reveals that the seawater of the Neotethys Ocean has penetrated into the central Africa during the period of Late Cretaceous global transgression.

# 2. Geological setting

The Central-West African Rift System can be obviously divided into two rift systems, namely, the West African Rift System and the Central African Rift System. The most prominent difference between the two rift systems is that the West African Rift System basins experienced transgression events in the Late Cretaceous and developed a set of marine sedimentary strata (e.g., the Termit Basin), while the Central African Rift System basins only deposited continental sedimentary sequences, such as the Muglad Basin (Fig. 1) (Fairhead, 1988; Schull, 1988; Genik, 1993). The Muglad Basin experienced three rifting episodes, which are the first syn-rift stage of the Barremian-Aptian during the Early Cretaceous, the second syn-rift stage of the Santonian-Maastrichtian during the Late Cretaceous, and third syn-rift stage during the Cenozoic Eocene to Oligocene (Fairhead, 1988; Guiraud and Maurin, 1992; McHargue et al., 1992). A group of the Cretaceous-Tertiary nonmarine sediments were unconformably deposited on the Pre-Cambrian basement rock (Fig. 2) (Schull, 1988). The Lower

Cretaceous sequences consist of thick lacustrine shale and marginal lacustrine mudstone, interbedded with a series of delta-facies fine sandstone beds, whereas the Upper Cretaceous sequences are interbedded marginal lacustrine and fluvial-deltaic sandstone and claystone (Guiraud and Maurin, 1992; McHargue et al., 1992). The organic-rich lacustrine shale in the Lower Cretaceous Barremian-Aptian lacustrine sediment (Abu Gabra Formation) is the only effective source rock for all discovered hydrocarbons (Makeen et al., 2015; Xiao et al., 2021). Much of more detailed basic geological setting on the Muglad Basin has previously been summarized in numerous references (Fairhead, 1988; Schull, 1988; Mohamed et al., 2002; Dou et al., 2013; Fadul Abul Gebbayin et al., 2018; Yassin et al., 2018; Xiao et al., 2021).

## 3. Samples and experimental

# 3.1. Rock samples

Nine representative rock samples were collected from the Lower Cretaceous Barremian-Aptian Formation (Abu Gabra Formation), while other two were collected from the Upper Cretaceous, one from the Santonian Formation (Aradeiba Formation) of the Hilba C-1 well and the other one from the Maastrichtian Formation (Baraka Formation) of the Abanose G-1 well. All collected rock samples are black drill cuttings. Before conducting geological experiments, we need to select the effective rock cuttings and wash them multiple times with distilled water to remove the contaminant covering the rock surface. The Abu Gabra Formation rock samples have the total organic carbon (TOC) content in the ranges of 1.00%—3.82% and the  $T_{\rm max}$  values in the range of 434–450 °C. The Upper Cretaceous rock samples collected from the Hilba C-1 and Abanose G-1 wells exhibit moderate organic matter abundance with the TOC values of 1.04% and 1.10%, respectively. The Tmax values of the two samples are relatively low, at 429 °C and 435 °C, respectively.

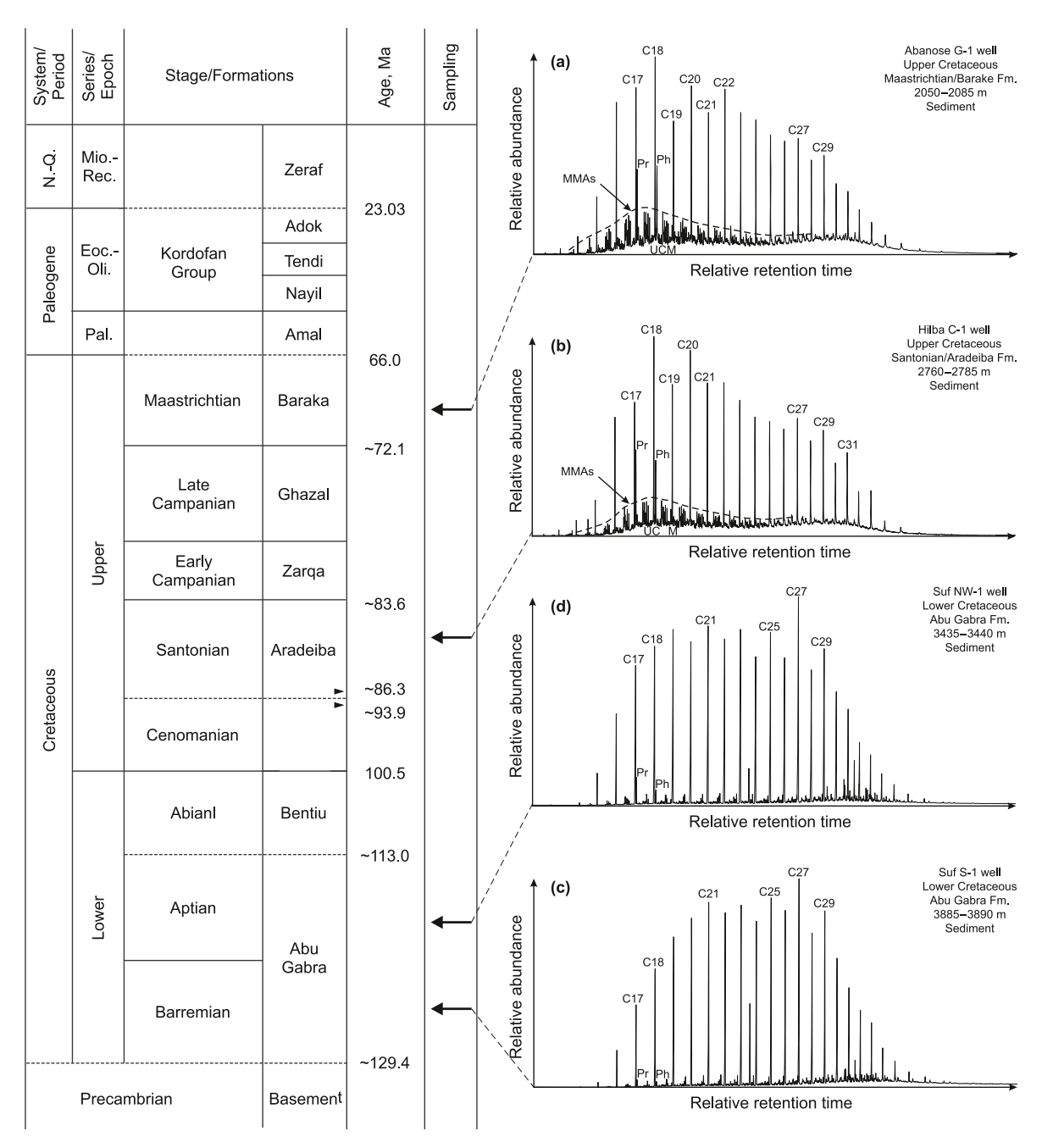


Fig. 2. Representative total ion chromatogram of saturated hydrocarbon of the Upper ((a)—(b)) and Lower Cretaceous sediments ((c)—(d)). Notes: MMAs = monomethyl alkanes; UCM = unresolved complex mixture.

# 3.2. Soluble hydrocarbon extraction and fractionation

All mudstone samples were pre-treated by washing with distilled water, drying at low-temperature in an oven, and then crushing them to a diameter of <0.2 mm (80 mesh). The extractable organic matter (EOM) was extracted from 50 to 70 g powder samples using a Soxhlet apparatus with 300 mL dichloromethane and methanol (93:7, v/v). Then, the EOM was dissolved in 50 mL petroleum ether and then poured into a funnel filled with degreased cotton to remove asphaltenes and the filtrate was collected. Finally, the filtrate was poured into a silica gel/alumina standard chromatography column. Petroleum ether, mixed reagent of dichloromethane and petroleum ether (2:1, v/v), and mixed

reagent of dichloromethane and methanol (93:7, v/v) were added sequentially to obtain saturated hydrocarbon, aromatic hydrocarbon and resin fractions, respectively.

# 3.3. Gas chromatography-mass spectrometry analysis

Molecular markers were analyzed by gas chromatography-mass spectrometry (GC–MS) on an Agilent 6890 gas chromatograph and an Agilent Model 5975i mass selective detector equipped with a HP-5 MS fused silica capillary column. For the saturated fractions, the initial GC oven temperature was set at 50 °C, maintained for 1 min, then increased to 120 °C at a rate of 20 °C/min and further to 310 °C at 3 °C/min, and finally maintained at 310 °C for 25 min. For

the aromatic fractions, the initial temperature of GC oven was also set at 50 °C, maintained for 1 min, then gradually increased to 310 °C at a rate of 3 °C/min, and the final temperature sequentially for 16 min. During these experiments, helium was used as a carrier gas. The MS was operated in electron impact with an ionization energy of 70 eV, and a scanning range of 50–600 Da. The samples cover a narrow value range of low thermal maturity (Makeen et al., 2015; Xiao et al., 2019a), therefore maturity differences are unlikely to account for differences in molecular signatures in our samples.

## 4. Results and discussion

#### 4.1. Biomarker analyses

#### 4.1.1. Total ion chromatogram

Normal alkanes (n-alkanes) are often used to indicate the organic matter sources and depositional environments. For instance, the high abundance and odd preference of long-chain nalkanes are always attributed to stronger inputs of terrigenous material inputs or low thermal maturity, whereas abundant shortchain *n*-alkanes suggest significant contribution of marine algae and/or bacteria (Moldowan et al., 1985; Li et al., 2007). The relative abundances of the high molecular weight n-alkanes (> $nC_{20}$ ) in typical marine-derived organic matter generally decrease with the increase of carbon number (Tissot et al., 1971). In the study, two main patterns for *n*-alkanes distribution indicate two major organo-facies groups. The Lower Cretaceous Barremian-Aptian sediments show the obvious odd preference and relative high abundance of long-chain n-alkanes, whereas the Upper Cretaceous Santonian-Maastrichtian sediments yield a predominance of  $nC_{22}$ over  $nC_{25}$  (Fig. 2). In most case, the thermal maturity of the lower sediments in the same basin should be slightly higher than that of the upper sediments. Therefore, the odd preference in the Lower Cretaceous Barremian-Aptian sediments (Fig. 2(c) and (d)) and the relatively higher abundance of short-chain *n*-alkanes in the Upper Cretaceous Santonian-Maastrichtian sediments (Fig. 2(a) and (b)) are considered to depend on organic matter inputs rather than thermal maturity. The even-to-odd preference of  $nC_{18}-nC_{22}$  in the Upper Cretaceous Santonian-Maastrichtian sediments may be related to brackish-saline sedimentary environments, which was also observed in the Upper Cretaceous marine marls and calcareous black shales from the Pará-Maranhão Basin in the western Brazil (Mello et al., 1988, 1989; De Grande et al., 1993). Similarly, lacustrine oils often show a waxy nature that is expressed for example in substantially higher  $nC_{27}/nC_{17}$  ratios compared to typical marine samples (Zumberge et al., 2000). The lower  $nC_{27}/nC_{17}$  ratio (<1) compared to the Lower Cretaceous samples (>> 1) thus points towards marine organic matter input to the Upper Cretaceous sediments.

The Upper Cretaceous samples show a markedly higher abundance of unresolved complex mixture (UCM) and monomethyl alkanes (MMAs) relative to the Lower Cretaceous samples (Fig. 2(a) and (b)). An elevated UCM is often the result of microbial degradation of liquid hydrocarbons in shallow reservoirs (Peters et al., 2005) and similarly more recalcitrant branched lipids could be enriched as a result of more intense microbial reworking either in the water column or during early diagenesis or as mild biodegradation upon petroleum formation (Pawlowska et al., 2013). The abundance of *n*-alkanes that are removed early during biodegradation would point more towards biological or early diagenetic sources of the more pronounced UCM and MMA-enrichment in the Upper Cretaceous Santonian-Maastrichtian sediments as typical for microbial reworking and in Proterozoic sediments (Summons et al., 1988; Kelly et al., 2011; Pawlowska et al., 2013; Bhattacharya et al., 2017). MMA maybe derived from cyanobacteria (Summons and

Walter, 1990) either through planktonic blooms or microbial mats in epicontinental sea ecosystems (Pawlowska et al., 2013).

# 4.1.2. Tricyclic terpanes

Tricyclic terpanes are among the best molecular predictors for depositional environments (Zumberge, 1987). Although multiple potential precursors for the tricyclic terpanes have been proposed. no clear precursor/product relationship has been established. Generally, marine sediments often show  $C_{23}TT$  as the predominant homologue among C<sub>19</sub>-C<sub>23</sub>TT (Aquino Neto et al., 1983) and marine-derived oils are typically enriched in C24TT and C25TT (Zumberge, 1987). The short-chain tricyclic terpanes ( $C_{19}$ – $C_{20}$ TT) were found to mainly be enriched in coal-bearing strata and/or terrestrial sediments rich in higher plant inputs (Aquino Neto et al., 1982), while the freshwater to brackish lacustrine samples are characterized by a dominance of C<sub>21</sub>TT (Xiao et al., 2019b, 2024). In crude oils, C<sub>21</sub>TT are similarly correlated with lacustrine, C<sub>19</sub>TT and C<sub>20</sub>TT with paralic/deltaic and C<sub>23</sub>TT to C<sub>25</sub>TT with marine depositional conditions (Zumberge, 1987). Moreover, all analyzed samples are in the low to mature thermal evolution stage, so the influence of thermal maturity on the distribution pattern of C<sub>19</sub>-C<sub>23</sub>TT can be ignored (Xiao et al., 2024). In the Muglad Basin, the Lower Cretaceous Barremian-Aptian lacustrine sediments show expected TT distributions, with C21TT as the major homologue (Fig. 3(c) and (d)). In contrast, the Upper Cretaceous Santonian-Maastrichtian sediments show typical marine facies feature with C<sub>23</sub>TT as the major homologue and relatively abundant of C<sub>24</sub>TT and C<sub>25</sub>TT (Fig. 3(a) and (b)), which is similar to the Upper Cretaceous marine sediments in the African Termit Basin (Xiao et al., 2019c). According to the C<sub>19</sub>-C<sub>23</sub>TT ternary diagram of sedimentary environments identification and previous analysis of marine and nonmarine samples from African basins (Xiao et al., 2019c), the two Upper Cretaceous samples were clearly distributed in marine setting (Zone I), consistent with the marine samples of the African Termit Basin, while the Lower Cretaceous samples were located in lacustrine area (Zone II) (Fig. 4).

In addition, the distribution patterns of high carbon number tricyclic terpanes are also quite different between the Lower and Upper Cretaceous sediments (Fig. 3(e)–(h)). For instance, in the Lower Cretaceous Barremian-Aptian lacustrine sediments, the abundance of C<sub>21</sub>TT to C<sub>29</sub>TT show a steady decreasing trend with very low abundance of  $C_{28}-C_{29}TT$  (Fig. 3(g) and (h)). The Upper Cretaceous Santonian-Maastrichtian sediments show extremely high abundance of C<sub>28</sub>-C<sub>29</sub>TT, which even exceeds C<sub>23</sub>TT (Fig. 3(e) and (f)). Although the reason for the high abundance of C<sub>28</sub>-C<sub>29</sub>TT is still controversial (e.g., maturity and/or biological sources) (Kruge et al., 1990), long chain tricyclic terpanes are often prominent in saline lacustrine and marine settings, such as the Hartford Basin, Brazilian and West African Marginal basins (Mello et al., 1988, 1989; Kruge et al., 1990; De Grande et al., 1993). Therefore, the high abundance of C28-C29TT in the Upper Cretaceous Santonian-Maastrichtian sediments is likely a product of marine transgression.

# 4.1.3. Pentacyclic terpanes

Generally, high abundance of  $C_{35}$  hopanes is attributed to strongly reducing conditions or high salinity lacustrine conditions (Peters and Moldowan, 1991; Hao et al., 2011), such as encountered in the upper fourth member sediment of the Eocene Shahejie Formation in the Dongying Depression, China (Li et al., 2003; You et al., 2020). In the current study, the relative abundance of  $C_{31}$ — $C_{35}$  homohopanes in both the Upper and Lower Cretaceous sediments show a gradual decrease pattern (Fig. 3(e)—(h)), indicating that both are not saline lacustrine environment.

Conventional perspective holds that the production of rearranged hopanes mainly depends on the clay-mediated acidic

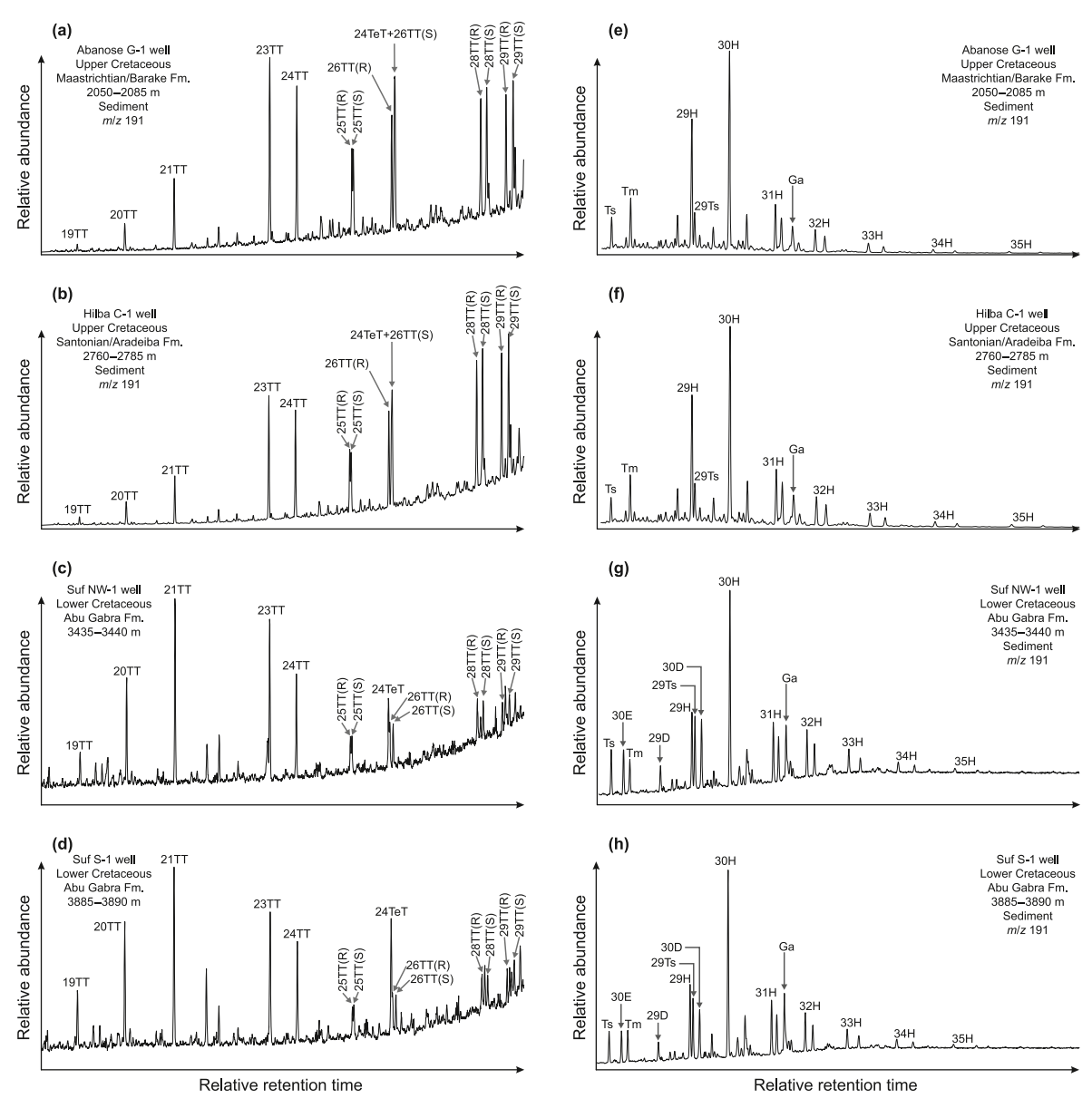


**Fig. 3.** Representative m/z 191 mass chromatograms showing the distribution of  $C_{19}$ - $C_{29}$  tricyclic terpanes and  $C_{24}$  tetracyclic terpane in the Lower (**(a)**-**(b)**) and Upper Cretaceous sediments (**(c)**-**(d)**), and the distribution of the hopane series in the Lower (**(e)**-**(f)**) and Upper Cretaceous sediments (**(g)**-**(h)**).

catalysis and oxic-suboxic conditions (Moldowan et al., 1991), but it may also be related to contribution of terrigenous higher plants because of their wide occurrence in coals and swamp sediments (Philp and Gilbert, 1986). In the current study, the Lower Cretaceous Barremian-Aptian lacustrine sediments contain abundant rearranged hopanes, mainly including early-eluting rearranged hopane  $(C_{30}E)$  and  $17\alpha(H)$ -diahopanes (e.g.,  $C_{29}D$  and  $C_{30}D$ ) (Fig. 3(g) and (h)). This scenario indicates a clay-rich sedimentary environment under oxic-suboxic conditions and/or large terrigenous material inputs, which is similar to the results exhibited by n-alkanes distribution pattern and  $Pr/Ph \gg 1.0$  (Xiao et al., 2019a). Considering that Ts and Tm that are often associated with clay catalysis do not show a similar enrichment in the Lower Cretaceous rocks, the marked enrichment of C<sub>30</sub>E and C<sub>30</sub>D is likely related to specific source inputs rather than differences in the diagenetic conditions/ extent of clay catalysis.

The absence or low abundance of rearranged hopanes in the Upper Cretaceous Santonian-Maastrichtian sediments (Fig. 3(e)

and (f)) may indicate a clay-poor sedimentary environment with low terrigenous organic matter input.

#### 4.1.4. Regular steranes and diasteranes

Steroids as the diagenetic products of sterols from membrane component of eukaryotes can be indicator for organic matter sources (Peters et al., 2005; Liu et al., 2010; Zhang et al., 2010). The Lower Cretaceous Barremian-Aptian lacustrine sediments show V-shaped distribution of  $C_{27}$ – $C_{29}$  regular steranes indicating mixed organism inputs (Fig. 5(c) and (d)), which is consistent with the distribution characteristics of n-alkanes with a bell-shaped pattern and  $C_{25}$ – $C_{29}$  odd-even preference (Fig. 2(c) and (d)). High abundance of diasteranes further suggests a clay-rich and oxic to suboxic conditions and/or a large amount of higher plants inputs (Fig. 5(c) and (d)) (Rubinstein et al., 1975; van Kaam-Peters et al., 1998; Peters et al., 2005). However, the Upper Cretaceous Santonian-Maastrichtian sediments show the predominance of  $C_{27}$  regular steranes (Fig. 5(a) and (b)), which reveals different organic

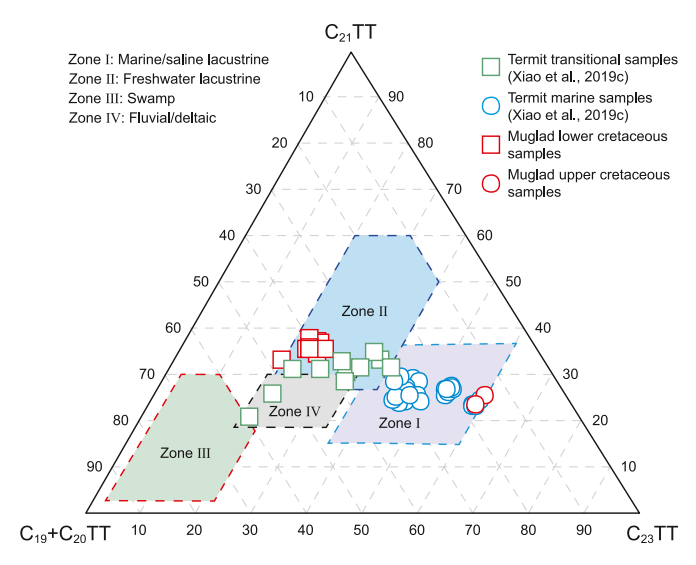


**Fig. 4.** A ternary diagram of  $C_{19}+C_{20}TT\%$ ,  $C_{21}TT\%$  and  $C_{23}TT\%$  to discriminate the various depositional environments (Xiao et al., 2024).

facies with high contribution of aquatic eukaryotic algae, consistent with a higher relative abundance of  $nC_{17}$  (Fig. 2(a) and (b)). Generally, the red algae and dinoflagellates containing  $C_{27}$  sterols are abundant in marine environments (Goodwin, 1973), which can make a substantial contribution to primitive organic matter of the

marine planktonic algal biomass (Moldowan et al., 1985). The regular steranes/17 $\alpha$ -hopanes ratio (St/H) can reflect the relative contributions of eukaryotes versus prokaryotes to the sedimentary organic matters. Marine sediments often have high St/H values, while the terrestrial organic matter always shows low values (Peters et al., 2005). In the current study, the St/H values of the two Upper Cretaceous Santonian-Maastrichtian sediments (0.30–0.35) are significantly higher than that of the nine Lower Cretaceous Barremian-Aptian lacustrine sediments (0.10–0.12), indicating a higher contribution of algae to the Upper Cretaceous sediments, consistent with marine depositional conditions.

#### 4.1.5. Dinosteranes

Dinosteranes ( $C_{30}$  4 $\alpha$ ,23,24-trimethylcholestanes) are derived predominantly from dinosterol or dinostanol synthesized by dinoflagellates (Withers, 1983). This series of compounds is usually abundant in marine sediments since the Late Triassic, which coincides with the appearance of fossil dinoflagellate cysts. Thus, dinosteranes can be used to constrain marine depositional environments (Summons et al., 1987, 1992; Li et al., 2010). Although dinosteranes and its isomer 4 $\alpha$ -methyl-24-ethyl-cholestanes could co-occur in marine sediments (Moldowan et al., 1985; Summons et al., 1987; Goodwin et al., 1988), the lacustrine sediments usually only contain 4 $\alpha$ -methyl-24-ethyl-cholestanes (Summons et al., 1992; Peters et al., 2005). Therefore, the presence of dinosteranes in sediments can be suggested as diagnostic molecular fossils for marine dinoflagellate inputs. According to the representative m/z 231 mass chromatograms, dinosteranes are virtually absent in the

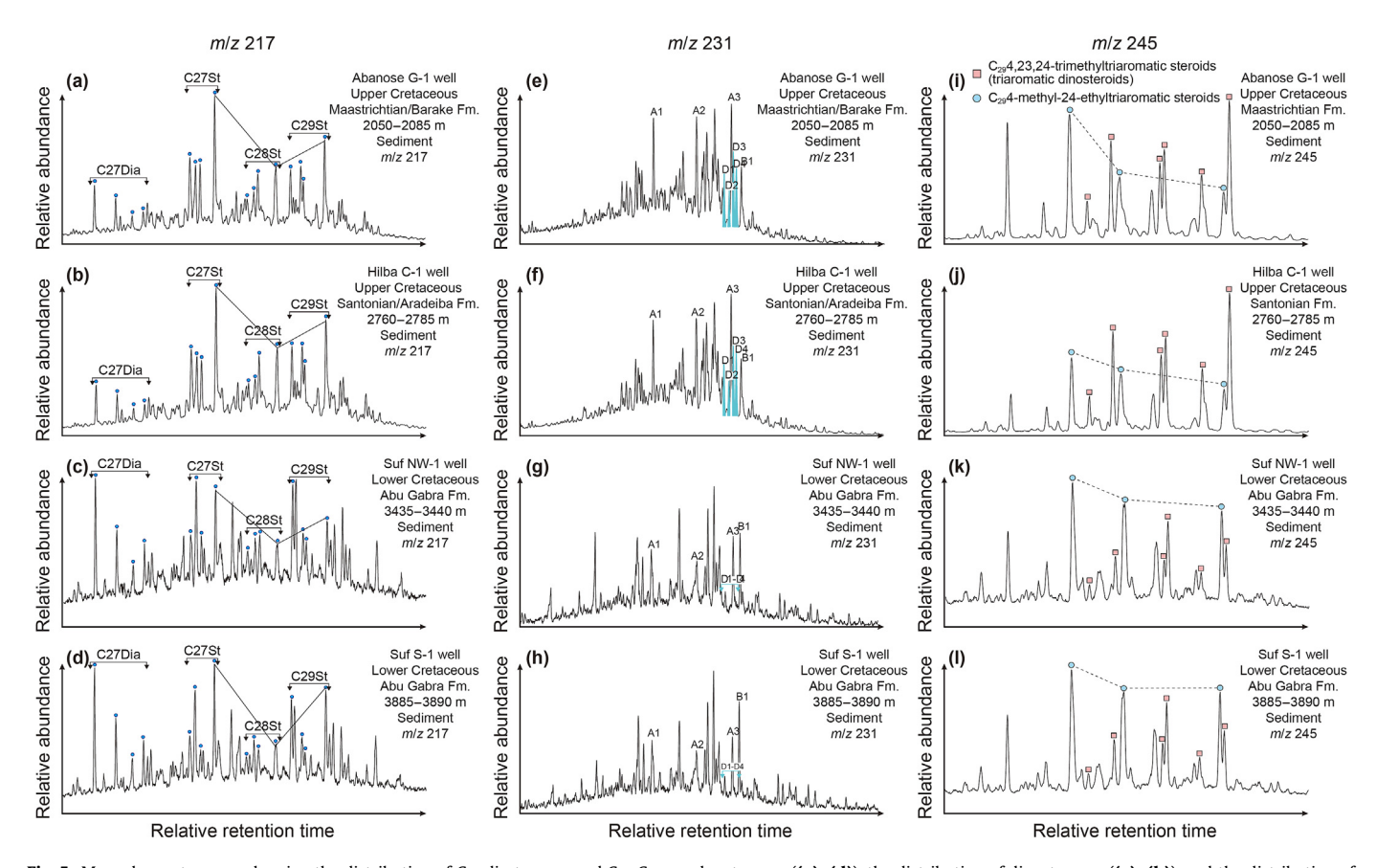


**Fig. 5.** Mass chromatograms showing the distribution of  $C_{27}$  diasteranes and  $C_{27}$ - $C_{29}$  regular steranes ((**a**)–(**d**)), the distribution of dinosteranes ((**e**)–(**h**)), and the distribution of methyl triaromatic steroids ((**i**)–(**1**)). Notes: A1 =  $C_{28}$  4α-methyl-cholestane (20R); A2 =  $C_{29}$  4α-methyl-24-methyl-cholestane (20R); A3 =  $C_{30}$  4α-methyl-24-ethyl-cholestane (20R); B1 =  $C_{30}$  hopane; D1 =  $C_{30}$  hopane; D1 =  $C_{30}$  4α-methyl-24-ethyl-cholestane; D2 =  $C_{30}$  4α-methyl-24-ethyl-cholestane; D3 =  $C_{30}$  4α-methyl-24-ethyl-cholestane; D4 =  $C_{30}$  4α-methyl-cholestane; D4 =  $C_{30}$  4α-methyl-cholestane;

Lower Cretaceous sediments, which is consistent with the lacustrine sedimentary environment (Fig. 5(g) and (h)). However, in the Upper Cretaceous sediments, four isomers of dinosteranes, namely 20R-4 $\alpha$ ,23S,24S-, 20R-4 $\alpha$ ,23S,24R-, 20R-4 $\alpha$ ,23R,24R- and 20R-4 $\alpha$ ,23R,24S-trimethylcholestanes, were detected (Fig. 5(e) and (f)). In order to more accurately identify these dinosteranes, it is necessary to compare their mass spectra and elution positions with previous publications (Summons et al., 1987; Goodwin et al., 1988; Hou et al., 2000). Generally, the elution positions of dinosteranes are always after C<sub>29</sub>  $\alpha\alpha\alpha$  regular sterane (Hou et al., 2000). Background subtracted mass spectra shows that the four dinosteranes have largely similar mass spectra, containing m/z 231 as a base peak and a molecular ion peak of M<sup>+</sup> 414, and diagnostic ion fragments at m/z 399, 98, 123, 163, 290 (Fig. 6).

The presence of substantial dinosteranes in the Upper Cretaceous Santonian-Maastrichtian sediments reveals a significant contribution of marine dinoflagellates to the sedimentary organic matter. These molecular fossils also provide decisive evidences for the early Cenomanian and late Turonian-early Santonian marine transgressional events in the gigantic freshwater Lake Songliao (Hou et al., 2000). Moreover, Mello et al. (1988) and De Grande et al. (1993) found that the Cretaceous crude oils and sediments from non-marine environments in Brazil were devoid of dinosteranes, as opposed to markedly higher concentration in the Cretaceous marine sediments and related crude oils (Mello et al., 1988; De Grande et al., 1993). Accordingly, the abundant dinosteranes in the Upper Cretaceous Santonian-Maastrichtian sediments serve as strong evidence for the marine transgression in the Muglad Basin. Fig. 5(e)—(h) also re-iterates the higher abundance of steranes relative to hopane in the Upper Cretaceous sediments where the 4methyl steranes (compounds A1-A3) are much larger than the  $C_{30}$ hopane (compound B1), and even dinosteranes (compounds D1-D4) exhibit similar peak heights as C<sub>30</sub> hopane, whereas in the Lower Cretaceous samples,  $C_{30}$  hopane is equal to or higher than A1-A3 and D1-D4 are virtually absent.

# 4.1.6. Triaromatic dinosteroids

Triaromatic dinosteroids was proposed to originate from dinosterol or structurally related 4,23,24-trimethycholesterols and indicate the biological origin of marine dinoflagellates, which can also serve as age- and source-related molecular (Peters et al., 2005). The undisputed oldest fossil of dinoflagellate cysts was observed in Middle Triassic sediments, and their concentrations in the vast majority of pre-Triassic marine sediments and related oils are always below detection limits, while are abundant in the Mesozoic marine samples (Moldowan et al., 1996).

In this study, the methyl triaromatic steroids exhibits sharply different distribution patterns between the Lower and Upper Cretaceous sediments (Fig. 5(i)–(I)). The Lower Cretaceous Barremian-Aptian lacustrine sediments are enriched in  $C_{29}$  4-methyl-24-ethyltriaromatic steroids (Fig. 5(k) and (I)), while the Upper Cretaceous Santonian-Maastrichtian sediments are typically dominated by  $C_{29}$  4,23,24-trimethyltriaromatic steroids (triaromatic dinosteroids) (Fig. 5(i) and (j)). Generally, the elevated abundance of triaromatic dinosteroids in the Upper Cretaceous Santonian-Maastrichtian sediments indicates significant contribution of dinoflagellates as typical for marine sedimentary environments. Consistent with the tri- and pentacylic terpane patterns, we consider this elevated dinosteroid signal to reflect a southern extension of seawater from the Neotethys Ocean.

# 4.1.7. Comparison to other recent organic geochemical studies of Muglad Basin sediments

In a recent conference proceeding, Fadul Abul Gebbayin et al. (2019) reported specific molecular signatures of six Upper Cretaceous cutting samples (from wells Lo-1, Zna-1 and Tim-1) and

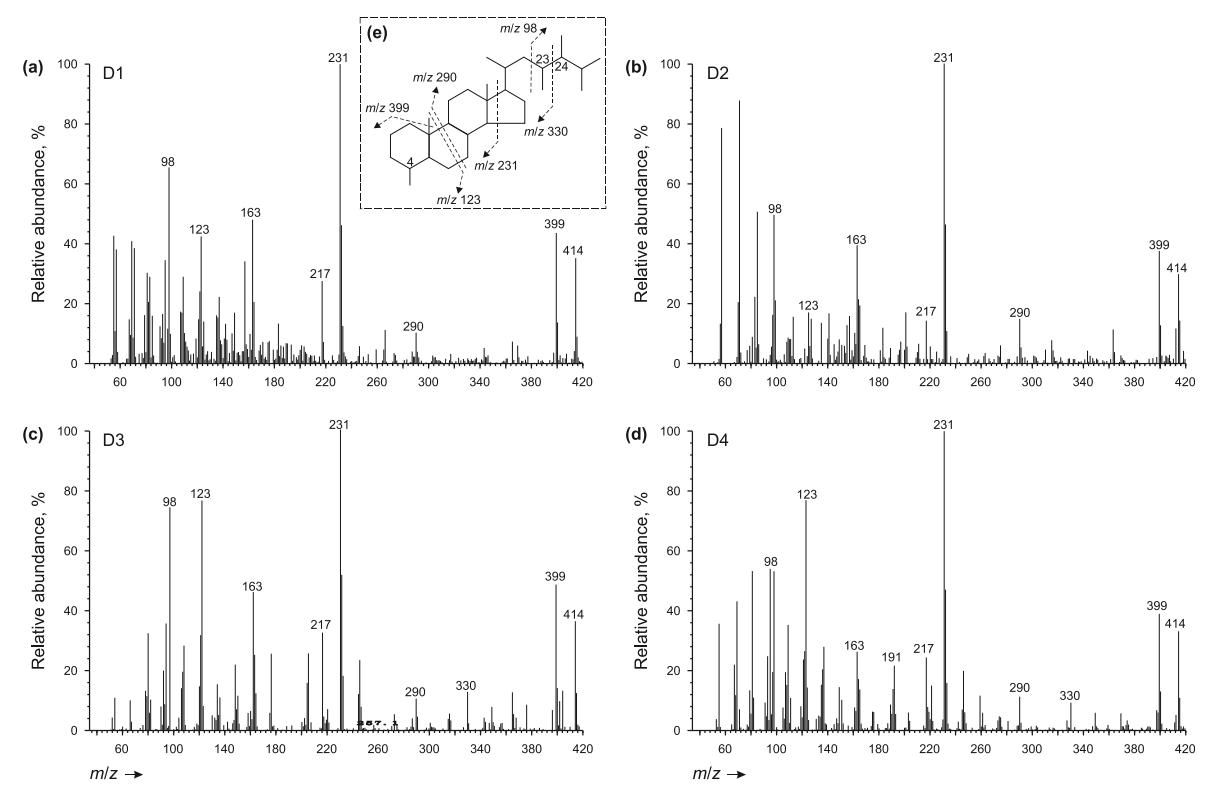


**Fig. 6.** Mass spectra of  $4\alpha$ ,23,24-trimethylcholestanes (dinosteranes) isomers. Peak positions of D1-D4 compounds are shown in Fig. 5(e) and (f). Notes: D1 = 20R- $4\alpha$ ,23S,24S-trimethylcholestane; D2 =  $20R-4\alpha$ ,23S,24R-trimethylcholestane; D3 =  $20R-4\alpha$ ,23R,24R-trimethylcholestane; D4 =  $20R-4\alpha$ ,23R,24S-trimethylcholestane.

compared them to eight cutting samples from the Lower Cretaceous Abu Gaba Formation (in wells ET-6, Nm K-2, Nm D-1 and Nm K-1). Based on substantial differences in the degree of waxiness, Pr/Ph ratios, tri-, tetra- and pentacyclic terpane and sterane distributions, they proposed a marine depositional environment for the Upper Cretaceous sediments. The results from the analyses of Fadul Abul Gebbayin and colleagues match those from our analyses that confirm the marine interpretations of Fadul Abul Gebbayin et al. (2019). The combined results encompassing sediments from the northern and southern parts of the basin point towards frequent or long-lasting marine incursions encompassing almost the full length of the basin.

#### 4.2. Paleogeographic evidence

During the Cretaceous period, the late Paleozoic-early Mesozoic supercontinent of Pangaea completed its breakup into present continents. Because of the expanding mid-oceanic ridges and intense volcanic activity (Larson, 1991), a large amount of CO<sub>2</sub> was emitted into the atmosphere, which further provoked global greenhouse conditions (Tarduno et al., 1998; Bice et al., 2006). Temperatures consequently increased until the end of the period resulting eventually in rising sea-level. At the peak of the Cretaceous transgression, nearly one-third of globe present land area was covered with warm epicontinental sea (Larson, 1991; Wang et al., 2005), such as the north Africa, north America and northwest Europe (Matsumoto, 1980).

Fig. 7(a) shows the global paleogeographic features of the Early-Late Cretaceous boundary (~90 Ma) published by Colorado Plateau Geosystems, Inc. At this time, the African continent suffered twoway transgressions from the northern Neotethys Ocean and the western South Atlantic Ocean, causing the basins located in the north of Africa (e.g., northern Algeria, Sirt and Western Desert basins) and the west part of the Central African Shear Zone (e.g., Termit Basin) to evolve into the epicontinental sea environments, while the Muglad Basin in Central African, located in the middle of the Central African Shear Zone, is still a lacustrine sedimentary setting without any transgression influences (Fig. 7(a)). In the past 100 million years, the overall geodynamic topography of the Central Africa continent was relatively high (Lithgow-Bertelloni and Silver, 1998; Daradich et al., 2003; Barnett-Moore et al., 2017), which was generally expressed in terrestrial sedimentary environments. During the period of Late Carboniferous to the Early Permian, the Hercynian tectonic deformation led to the formation of uplift-depression framework and a series of nearly south-north trend basins in the North Africa (Vail et al., 1977; Faqira et al., 2009). Until the Mesozoic Era, the Neotethys Ocean began to expand and gradually transgressed into the Africa continent. When the global sea level rose to the highest level during the Late Cretaceous (Vail et al., 1977), a large area of the North Africa continent was submerged and formed the extensive epicontinental sea sedimentary environments (Guiraud et al., 2005). Under the geological background of an uplift-depression framework formed in the Hercynian Orogeny and the global largest scale transgression, the Neotethys seawater can be expected to have invade into the Muglad Basin through the residual north-south troughs in the Late Cretaceous as predicted by the deep time map (Fig. 7(b)), and confirmed by the marine molecular traces in the Upper Cretaceous sediments of the Muglad Basin discovered in the present study (Figs. 2–5). This process is very similar to the Niger Termit Basin of the West African Rift System. The Neotethys seawater poured southward into the Termit basin through the troughs in Mali and Algeria (Fig. 7(b)), making the basin widely develop a set of marine sedimentary strata in the Late Cretaceous (i.e., the Upper Cretaceous Yogou Formation) (Guiraud et al., 2005).

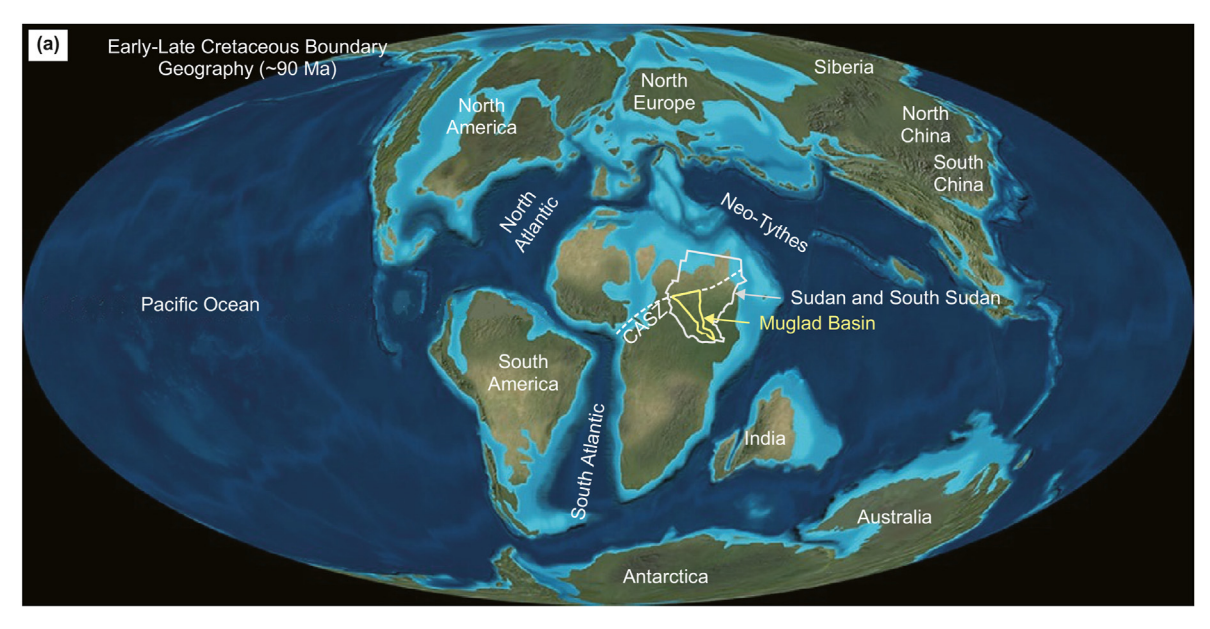
According to the stratigraphic ages of the limited samples in the study, it can be determined that the transgression of the Neotethys Ocean into the Muglad Basin already began in the Santonian age (between 86.3 and 83.6 Ma) at the latest and likely sometime after the Aptian period (<113.0 Ma) from which we exclusively recovered non-marine molecular signatures in both source rocks and crude oils (Xiao et al., 2019a).

## 4.3. Paleontological evidence

Additional strong paleontological evidence for marine depositional conditions comes from two dinoflagellates species, namely xochosphaeridium/Downiesphaeridium (Fig. 8(b) and (c)) and Spicadinium sp. cf. S. nenjiangense groups (Fig. 8(c) and (d)), which have been identified at the bottom sections of the Upper Cretaceous sediments from the Kng W-1 well in the Muglad Basin (Fadul Abul Gebbayin et al., 2019). Although dinoflagellate species could thrive in both marine and lacustrine sedimentary environments (Fu et al., 1990), the lacustrine dinoflagellate communities often only produce C<sub>30</sub> 4α-methyl-24-ethyl-cholestane fossils, while marine dinoflagellates can form abundant C<sub>30</sub> 4,23,24-trimethylcholestane (dinosteranes) (Summons et al., 1987, 1992; Goodwin et al., 1988). The Kng W-1 well is situated in the south of the Kaikang Trough, while the Hilba C-1 and the Abanose G-1 wells are situated in the north (Fig. 8(a)). As shown in Fig. 1, the Neotethys Ocean is located on the north side of the African continent, so the direction of seawater intrusion into the Muglad Basin must be from the north (Fig. 8(a)) and seawater would have gradually inundated the basin from north to south. In other words, if the Upper Cretaceous sediment of the Kng W-1 well in the south was affected by seawater, that of the Hilba C-1 and the Abanose G-1 wells in the north must be also affected. Consequently, the co-occurrence of dinoflagellate body fossils (Fig. 8) and dinosteranes/triaromatic dinosteroids molecular fossils in the Upper Cretaceous Santonian-Maastrichtian sediments (Fig. 5) reveals that the Muglad Basin developed a shallow marine sedimentary environment with dinoflagellate algae flourishing during the Late Cretaceous. The occurrence of marine dinoflagellates in well Kng W-1 in the southern Muglad Basin (Figs. 7(b) and 8(a)) and the marine biomarker signatures reported by Fadul Abul Gebbayin et al. (2019) for close-by wells Lo-1 and Zna-1 would further indicate that, at least at times, the Neotethys expanded even further into the African continent than predicted by the deep time map (Fig. 7(b)).

# 4.4. Lithological evidence

The circulation of seawater through the enlarged ridges during Cretaceous is thought to have saturated the oceans in calcium. High concentration of calcium promotes the prosperity of calcareous nanoplankton (e.g., coccolithophores) in Cretaceous seas, forming the most famous chalk composed of coccoliths and calcite skeleton of coccolithophores. Interestingly, Fadul Abul Gebbayin et al. (2019) reported that calcareous and chalky strata with a thickness of almost 400 m were observed in the top of the Late Cretaceous Baraka Formation (Maastrichtian) of the Tmr-1 well in the Muglad Basin (Fig. 8(a)) (Fadul Abul Gebbayin et al., 2019), which serves as a lithological indicator for seawater incursion during the Late Cretaceous. Moreover, a submarine fan deposit thought to represent a marine sedimentary environment was also observed in the Aradeiba Formation (Santonian) of Muglad Basin (Fadul Abul Gebbayin et al., 2019). Consistent with the widespread occurrence of marine molecular signatures of Upper Cretaceous sediments throughout the basin, the reported extent of the chalky strata points towards frequent or long-lasting marine incursions into the Muglad Basin during the Late Cretaceous period.



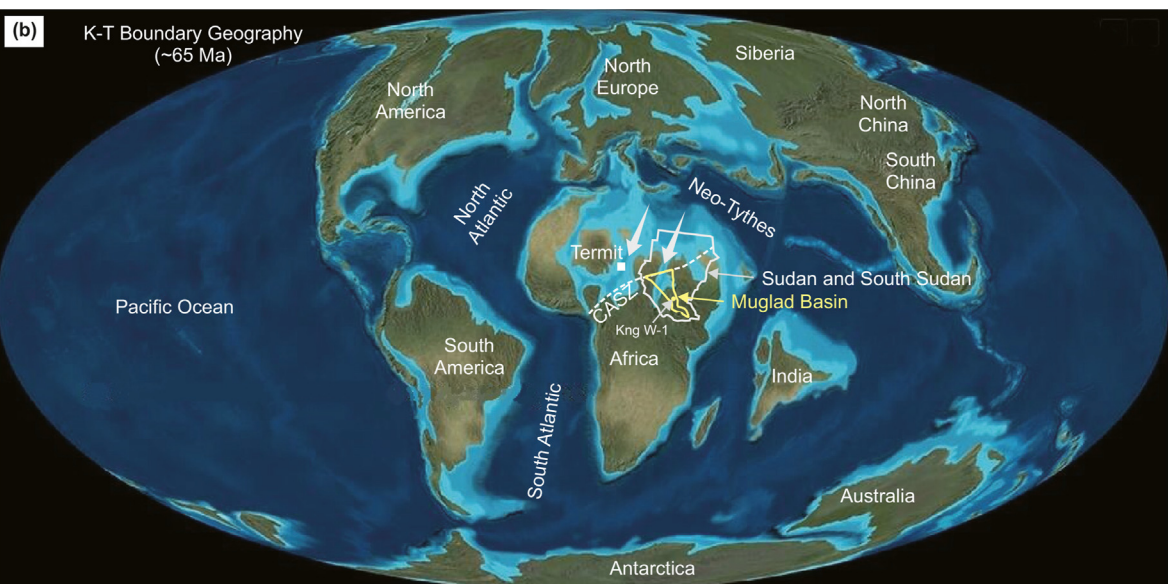


Fig. 7. Late Cretaceous paleogeography of the globe and location of the Muglad Basin (Modified from: Deep Time Maps, produced by Colorado Plateau Geosystems, Inc.).

# 4.5. Implication for future petroleum exploration

As a Mesozoic-Cenozoic continental basin, the Muglad Basin has long been believed to have only developed a set of organic-rich source rock, namely the Lower Cretaceous Abu Gabra Formation lacustrine shale (Makeen et al., 2015; Xiao et al., 2021). All discovered oils in the basin are derived from the Abu Gabra Formation source rock and belong to one oil family (Makeen et al., 2015). However, this study firstly determined the presence of organic-rich marine sediments within the Upper Cretaceous Darfur Group in the Muglad Basin, which reveals that the study area not only develops lacustrine source rock, but also potential marine source rock. Moreover, Xiao et al. (2019a) also have reported an outlier oil sample from the Kela-1 well in the basin, which contains completely different biomarker compositions from all discovered lacustrinesource oils, including tricyclic terpanes, tetracyclic terpanes, regular steranes,  $4\alpha$ -methylsteranes, diasteranes and diahopanes. Based on the results of oil-source rock correlation analysis, it is determined

that the Kela-1 oil originates from the Darfur Group marine sediment and can be divided into a new oil family (Xiao et al., 2019a), which can be referred to as the marine-source oil family to distinguish it from the lacustrine-source oil family.

The TOC values of the Upper Cretaceous Darfur Group mudstone samples from the Hilba C-1 and Abanose G-1 wells are 1.04% and 1.10%, respectively, both of which are greater than 1.0% and are generally considered as fair to good potential source rocks. Their Rock-Eval pyrolysis peak temperature ( $T_{\rm max}$ ) values are relatively low with a range of 429–435 °C, indicating the immature to low mature evolution stage. The moderate organic matter abundance and low thermal evolution maturity of the Darfur Group mudstone samples from the Hilba C-1 and Abanose G-1 wells are mainly controlled by the fact that these two wells are located in the slope zone or uplift zone of the basin, and the burial depth of source rock samples is relatively shallow (Xiao et al., 2019a). Generally, the Darfur Group source rock in the center of the depression is not only buried at a deeper depth than the Hilba C-1 and Abanose G-1 wells,

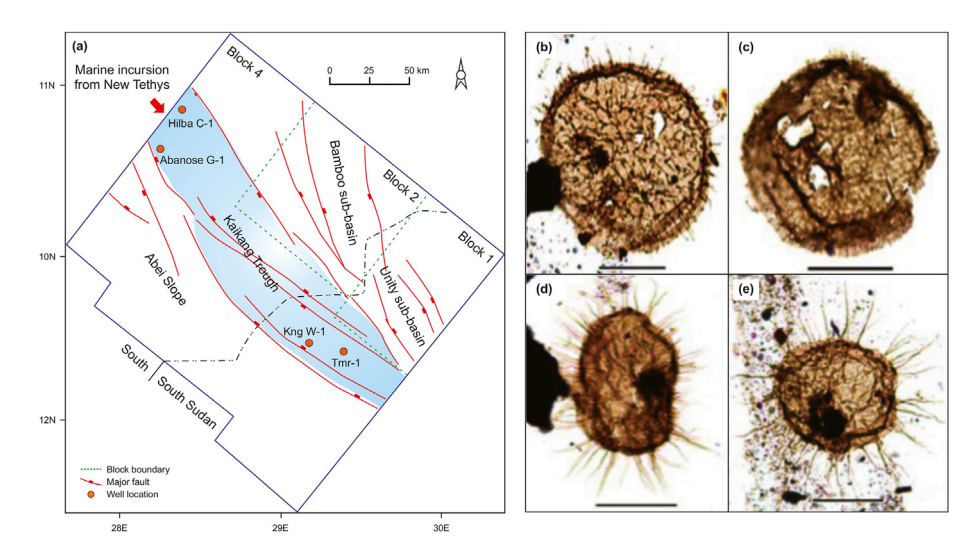


Fig. 8. The location of analyzed wells in the Kaikang Trough of the Muglad Basin (a), and two species of dinoflagellates in the Upper Cretaceous sediments from Kng W-1 well ((b)—(e)).

indicating that it has entered the main stage of hydrocarbon generation, but also likely to have higher organic matter abundance. Based on the quality of the Darfur Group source rock and the discovered related oil from the Kela-1 well, it can be inferred that the marine-source oil family in the Muglad Basin may be a new area for future oil exploration in the study area.

#### 5. Conclusion

This study found markedly different molecular marker assemblage in the Upper Cretaceous Santonian-Maastrichtian sediments compared to the Lower Cretaceous Barremian-Aptian freshwater lacustrine sediments. The proposed marine signatures mainly include the predominance of short-chain *n*-alkanes, abundant MMAs, dominant C<sub>23</sub>TT and abundant C<sub>28</sub>-C<sub>29</sub>TT, dominant C<sub>27</sub> regular steranes, and more importantly, the significant distribution of dinosteranes and triaromatic dinosteroids. We consider these special molecular markers in the Upper Cretaceous Santonian-Maastrichtian sediments to be the products of seawater incursion. Based on the comprehensive analyses of molecular fossils (e.g., dinosteranes and triaromatic dinosteroids), paleogeography (e.g., Deep Time Maps), paleontology (e.g., dinoflagellate fossils) and lithology (e.g., chalk deposits), we propose that the Muglad Basin received intermittent marine inundations during the Santonian-Maastrichtian stages. This finding redefines the southern limit of the Late Cretaceous transgression for the Africa continent.

# **CRediT authorship contribution statement**

**Hong Xiao:** Writing — review & editing, Writing — original draft, Resources, Methodology, Funding acquisition, Conceptualization. **Mei-Jun Li:** Supervision, Resources, Funding acquisition. **Benjamin J. Nettersheim:** Writing — review & editing, Methodology. **Bing You:** Writing — review & editing, Data curation. **Man Lu:** Methodology. **Ding-Sheng Cheng:** Funding acquisition.

# **Declaration of competing interest**

The authors declare that they have no known competing financial interests or personal relationships that could have appeared to influence the work reported in this paper.

# Acknowledgements

This work was supported by the National Natural Science Foundation of China (No. 42202134), Science Foundation of China University of Petroleum, Beijing (No. 2462023YJRC010) and the postdoctoral fellowship by the Central Research and Development Fund of the University of Bremen. The authors would like to thank the editor and the two anonymous reviewers for their constructive comments and suggestions which significantly improved the quality of the manuscript.

## References

An, K.X., Chen, H.L., Lin, X.B., 2017. Major transgression during Late Cretaceous constrained by basin sediments in northern Africa: implication for global rise in sea level. Front. Earth Sci. 11, 740–750. https://doi.org/10.1007/s11707-017-0661-0.

Aquino Neto, F.R., Restle, A., Connan, J., et al., 1982. Novel tricyclic terpanes (C<sub>19</sub>, C<sub>20</sub>) in sediments and petroleums. Tetrahedron Lett. 23, 2027–2030. https://doi.org/10.1016/S0040-4039(00)87251-2.

Aquino Neto, F.R., Trendel, J.M., Restlé, A., et al., 1983. Occurrence and formation of tricyclic terpanes in sediments and petroleums. In: Bjorøy, M., Albrecht, P., Cornford, C., de Groot, K., Eglinton, G., Galimov, E., Leythaeuser, D., Pelet, R., Rullkötter, J., Speers, G. (Eds.), Adv. Org. Geochem. 1981. Wiley, Chichester, pp. 659–667. https://doi.org/10.1016/0009-2541(85)90011-7.

Badalini, G., Redfern, J., Carr, I.D., 2006. Introduction - a synthesis of current understanding of the structural evolution of North Africa. J. Petrol. Geol. 25, 249–258. https://doi.org/10.1111/j.1747-5457.2002.tb00008.x.

Barnett-Moore, N., Hassan, R., Mueller, R.D., et al., 2017. Dynamic topography and eustasy controlled the paleogeographic evolution of northern Africa since the mid-Cretaceous. Tectonics 36, 929–944. https://doi.org/10.1002/2016TC004280.

Bhattacharya, S., Dutta, S., Summons, R.E., 2017. A distinctive biomarker assemblage in an Infracambrian oil and source rock from western India: molecular signatures of eukaryotic sterols and prokaryotic carotenoids. Precambr. Res. 290, 101–112. https://doi.org/10.1016/j.precamres.2016.12.013.

Bice, K.L., Birgel, D., Meyers, P.A., et al., 2006. A multiple proxy and model study of Cretaceous upper ocean temperatures and atmospheric CO<sub>2</sub> concentrations. Paleoceanography 21, 1–17. https://doi.org/10.1029/2005PA001203.

Daradich, A., Mitrovica, J.X., Pysklywec, R.N., et al., 2003. Mantle flow, dynamic topography, and rift-flank uplift of Arabia. Geology 31, 901–904. https://doi.org/10.1130/G19661.1.

De Grande, S.M.B., Aquino Neto, F.R., Mello, M.R., 1993. Extended tricyclic terpanes in sediments and petroleums. Org. Geochem. 20, 1039–1047. https://doi.org/10.1016/0146-6380(93)90112-0.

Dou, L.R., Cheng, D.S., Zhi, L., et al., 2013. Petroleum geology of the Fula sub-basin, Muglad Basin, Sudan. J. Petrol. Geol. 36, 43–59. https://doi.org/10.1111/ ipg 12541

Fadul Abul Gebbayin, O.I.M., Zhong, N.N., Ibrahim, G.A., et al., 2018. Origin of a Tertiary oil from El Mahafir wildcat & geochemical correlation to some Muglad source rocks, Muglad basin, Sudan. J. Afr. Earth Sci. 137, 133–148. https://

#### doi.org/10.1016/j.jafrearsci.2017.10.008.

- Fadul Abul Gebbayin, O.I.M., Zhong, N.N., Luo, Q.Y., et al., 2019. New insights on Muglad's Cretaceous source rocks: a paleo-geographic review & organic geochemical characterization, Muglad basin, Sudan. IOP Conf. Ser. Earth Environ. Sci. 360, 012030. https://doi.org/10.1088/1755-1315/360/1/012030.
- Fairhead, J.D., 1988. Mesozoic plate tectonic reconstructions of the central South Atlantic Ocean: the role of the West and Central African rift system. Tectonophysics 155, 181–191. https://doi.org/10.1016/0040-1951(88)90265-X.
- Faqira, M., Rademakers, M., Afifi, A.K.M., 2009. New insights into the hercynian Orogeny, and their implications for the paleozoic hydrocarbon system in the Arabian plate. GeoArabia (Manama) 14, 199–228. https://doi.org/10.2113/geoarabia1403199.
- Fu, J.M., Sheng, G.Y., Xu, J.Y., et al., 1990. Application of biological markers in the assessment of paleoenvironments of Chinese non-marine sediments. Org. Geochem. 16, 769–779. https://doi.org/10.1016/0146-6380(90)90116-H.
- Genik, G.J., 1993. Petroleum geology of Cretaceous-Tertiary rift basinsin Niger, Chad, and Central African Republic. AAPG Bull. 77, 1405–1434. https://doi.org/10.1306/BDFF8EAC-1718-11D7-8645000102C1865D.
- Goncuoglu, M.C., Kozlu, H., 2000. Early paleozoic evolution of the NW Gondwanaland: data from southern Turkey and surrounding regions. Gondwana Res. 3, 315–324. https://doi.org/10.1016/S1342-937X(05)70290-2.
- Goodwin, N.S., Mann, A.L., Patience, R.L., 1988. Structure and significance of C<sub>30</sub> 4-methyl steranes in lacustrine shales and oils. Org. Geochem. 12, 495–506. https://doi.org/10.1016/0146-6380(88)90159-3.
- Goodwin, T.W., 1973. Comparative biochemistry of sterols in eukaryotic microorganisms. In: Erwin, J.A. (Ed.), Lipids and Biomembranes of Eukaryotic Microorganisms. Academic Press, New York, pp. 1–40. https://doi.org/10.1016/B978-0-12-242050-4 50007-0
- Guiraud, R., Bosworth, W., Thierry, J., et al., 2005. Phanerozoic geological evolution of northern and central Africa: an overview. J. Afr. Earth Sci. 43, 83—143. https://doi.org/10.1016/j.jafrearsci.2005.07.017.
- Guiraud, R., Maurin, J.C., 1992. Early cretaceous rift of western and central Africa: an overview. Tectonophysics 213, 153–168. https://doi.org/10.1016/0040-1951(92) 90256-6.
- Hao, F., Zhou, X.H., Zhu, Y.M., et al., 2011. Lacustrine source rock deposition in response to co-evolution of environments and organisms controlled by tectonic subsidence and climate, Bohai Bay Basin, China. Org. Geochem. 42, 323–339. https://doi.org/10.1016/j.orggeochem.2011.01.010.
- Hou, D.J., Li, M.W., Huang, Q.H., 2000. Marine transgressional events in the gigantic freshwater lake Songliao: paleontological and geochemical evidence. Org. Geochem. 31, 763–768. https://doi.org/10.1016/S0146-6380(00)00065-6.
- Kelly, A.E., Love, G.D., Zumberge, J.E., et al., 2011. Hydrocarbon biomarkers of neoproterozoic to lower cambrian oils from eastern siberia. Org. Geochem. 42, 640–654. https://doi.org/10.1016/j.orggeochem.2011.03.028.
- Kruge, M.A., Hubert, J.F., Akes, R.J., et al., 1990. Biological markers in Lower Jurassic synrift lacustrine black shales, Hartford basin, Connecticut, U.S.A. Org. Geochem. 15, 281–289. https://doi.org/10.1016/0146-6380(90)90006-L.
- Larson, R.L., 1991. Latest pulse of Earth: Evidence for a mid-Cretaceous superplume. Geology 19, 547–550. https://doi.org/10.1130/0091-7613(1991)019<0547: LPOEFF 2 3 CO 2
- Li, M.J., Wang, T.G., Liu, J., et al., 2007. Characteristics of oil and gas accumulation in Yong'an-Meitai area of the Fushan Depression, Beibuwan Basin, South China Sea. Pet. Sci. 4, 23–33. https://doi.org/10.1007/BF03187452.
- Li, S.M., Pang, X.Q., Li, M.W., et al., 2003. Geochemistry of petroleum systems in the Niuzhuang South Slope of Bohai Bay Basin—part 1: source rock characterization. Org. Geochem. 34, 389–412. https://doi.org/10.1016/S0146-6380(02) 00210-3
- Li, S.M., Pang, X.Q., Zhang, B.S., et al., 2010. Oil-source rock correlation and quantitative assessment of Ordovician mixed oils in the Tazhong Uplift, Tarim Basin. Pet. Sci. 7, 179–191. https://doi.org/10.1007/s12182-010-0025-9.
- Lithgow-Bertelloni, C., Silver, P.G., 1998. Dynamic topography, plate driving forces and the African superswell. Nature 395, 269–272. https://doi.org/10.1038/26212.
- Liu, G.D., Gao, G., Huang, Z.L., et al., 2010. Oil source and accumulation in the overthrust belt in the Ke-Bai region, Junggar Basin, west China. Pet. Sci. 7, 31–39. https://doi.org/10.1007/s12182-010-0004-1.
- Lüning, S., Gräfe, K.-U., Bosence, D., Luciani, V., Craig, J., 2000. Discovery of marine Late Cretaceous carbonates and evaporites in the Kufra Basin (Libya) redefines the southern limit of the Late Cretaceous transgression. Cretac. Res. 21, 721–731. https://doi.org/10.1006/cres.2000.0231.
- Makeen, Y.M., Wan, H.A., Hakimi, M.H., et al., 2015. Source rock characteristics of the Lower Cretaceous Abu Gabra Formation in the Muglad Basin, Sudan, and its relevance to oil generation studies. Mar. Petrol. Geol. 59, 505–516. https:// doi.org/10.1016/j.marpetgeo.2014.09.018.
- Matsumoto, T., 1980. Inter-regional correlation of transgressions and regressions in the Cretaceous period. Cretac. Res. 1, 359–373. https://doi.org/10.1016/0195-6671(80)90044-0.
- McHargue, T.R., Heidrick, T.L., Livingston, J.E., 1992. Tectonostratigraphic development of the Interior Sudan rifts, Central Africa. Tectonophysics 213, 187–202. https://doi.org/10.1016/0040-1951(92)90258-8.
- Mello, M.R., Koutsoukos, E.A.M., Hart, M.B., et al., 1989. Late cretaceous anoxic events in the Brazilian continental margin. Org. Geochem. 14, 529–542. https:// doi.org/10.1016/0146-6380(89)90033-8.
- Mello, M.R., Telnaes, N., Gaglianone, P.C., et al., 1988. Organic geochemical characterisation of depositional palaeoenvironments of source rocks and oils in

- Brazilian marginal basins. Org. Geochem. 13, 31–45. https://doi.org/10.1016/0146-6380(88)90023-X.
- Miller, K.G., Kominz, M.A., Browning, J.V., et al., 2005. The Phanerozoic record of global sea-level change. Science 310, 1293–1298. https://doi.org/10.1126/science.1116412.
- Mohamed, A.Y., Pearson, M.J., Ashcroft, W.A., et al., 2002. Petroleum maturation modelling, Abu Gabra—Sharaf area, Muglad Basin, Sudan. J. Afr. Earth Sci. 35, 331–344. https://doi.org/10.1016/S0899-5362(01)00097-5.
- Moldowan, J.M., Dahl, J., Jacobson, S.R., et al., 1996. Chemostratigraphic reconstruction of biofacies: Molecular evidence linking cyst-forming dinoflagellates with pre-Triassic ancestors. Geology 24, 159–162. https://doi.org/10.1130/0091-7613(1996)024<0159:CROBME>2.3.CO;2.
- Moldowan, J.M., Fago, F.J., Carlson, R.M.K., et al., 1991. Rearranged hopanes in sediments and petroleum. Geochim. Cosmochim. Acta 55, 3333–3353. https://doi.org/10.1016/0016-7037(91)90492-N.
- Moldowan, J.M., Seifert, W.K., Gallegos, E.J., 1985. Relationship between petroleum composition and depositional environment of petroleum source rock. AAPG Bull. 69, 1255–1268. https://doi.org/10.1306/AD462BC8-16F7-11D7-8645000102C1865D.
- Pawlowska, M.M., Butterfield, N.J., Brocks, J.J., 2013. Lipid taphonomy in the Proterozoic and the effect of microbial mats on biomarker preservation. Geology 41, 103–106. https://doi.org/10.1130/G33525.1.
- Peters, K.E., Moldowan, J.M., 1991. Effects of source, thermal maturity, and biodegradation on the distribution and isomerization of homohopanes in petroleum. Org. Geochem. 17, 47–61. https://doi.org/10.1016/0146-6380(91) 90039-M.
- Peters, K.E., Walters, C.C., Moldowan, J.M., 2005. The Biomarker Guide: Biomarkers and Isotopes in Petroleum Exploration and Earth History, Second ed. vol 2. Cambridge University Press, Cambridge.
- Philp, R.P., Gilbert, T.D., 1986. Biomarker distributions in Australian oils predominantly derived from terrigenous source material. Org. Geochem. 10, 73–84. https://doi.org/10.1016/0146-6380(86)90010-0.
- Rubinstein, I., Sieskind, O., Albrecht, P., 1975. Rearranged sterenes in a shale: occurrence and simulated formation. J. Chem. Soc., Perkin Transactions 1, 1833–1836. https://doi.org/10.1039/p19750001833.
- Schull, T.J., 1988. Rift basins of interior Sudan: petroleum exploration and discovery. AAPG Bull. 72, 1128–1142. https://doi.org/10.1306/703C9965-1707-11D7-8645000102C1865D.
- Summons, R.E., Powell, T.G., Boreham, C.J., 1988. Petroleum geology and geochemistry of the Middle Proterozoic McArthur Basin, Northern Australia: III. Composition of extractable hydrocarbons. Geochim. Cosmochim. Acta 52, 1747–1763. https://doi.org/10.1016/0016-7037(88)90001-4.
- Summons, R.E., Thomas, J., Maxwell, J.R., et al., 1992. Secular and environmental constraints on the occurrence of dinosterane in sediments. Geochim. Cosmochim. Acta 56, 2437–2444. https://doi.org/10.1016/0016-7037(92)90200-3.
- Summons, R.E., Volkman, J.K., Boreham, C.J., 1987. Dinosterane and other steroidal hydrocarbons of dinoflagellate origin in sediments and petroleum. Geochim. Cosmochim. Acta 51, 3075—3082. https://doi.org/10.1016/0016-7037(87)90381-
- Summons, R.E., Walter, M.R., 1990. Molecular fossils and microfossils of prokaryotes and protists from Proterozoic sediments. Am. J. Sci. 290, 212–244. https://doi.org/10.1029/JB095iB01p00649.
- Tarduno, J.A., Brinkman, D.B., Renne, P.R., et al., 1998. Evidence for extreme climatic warmth from late cretaceous arctic vertebrates. Science 282, 2241–2244. https://doi.org/10.1126/science.282.5397.2241.
- Tissot, B., Califet-Debyser, Y., Deroo, G., et al., 1971. Origin and evolution of hydrocarbons in Early Toarcian shales, Paris Basin, France. AAPG Bull. 55, 2177—2193. https://doi.org/10.1306/819A3E2E-16C5-11D7-8645000102C1865D.
- Vail, P.R., Mitchum, R.M.J., Thompson, S.I., 1977. Seismic Stratigraphy and Global Changes of Sea Level, Part 4: Global Cycles of Relative Changes of Sea Level. AAPG Memoir, pp. 83–97. https://doi.org/10.1029/2002GL015986.
- van Kaam-Peters, H.M.E., Köster, J., van der Gaast, S.J., et al., 1998. The effect of clay minerals on diasterane/sterane ratios. Geochim. Cosmochim. Acta 62, 2923–2929. https://doi.org/10.1016/S0016-7037(98)00191-4.
- Veevers, J.J., 2004. Gondwanaland from 650–500 Ma assembly through 320 Ma merger in Pangea to 185–100 Ma breakup: supercontinental tectonics via stratigraphy and radiometric dating. Earth Sci. Rev. 68, 1–132. https://doi.org/10.1016/j.earscirev.2004.05.002.
- Wang, C., Hu, X., Sarti, M., et al., 2005. Upper Cretaceous oceanic red beds in southern Tibet: a major change from anoxic to oxic, deep-sea environments. Cretac. Res. 26, 21–32. https://doi.org/10.1016/j.cretres.2004.11.010.
- Withers, N., 1983. Dinoflagellate sterols. In: Scheuer, P.J. (Ed.), Marine Natural Products 5. Academic Press, New York, pp. 87–130.
- Xiao, H., Li, M.J., Liu, J.G., et al., 2019a. Oil-oil and oil-source rock correlations in the Muglad Basin, Sudan and South Sudan: New insights from molecular markers analyses. Mar. Petrol. Geol. 103, 351–365. https://doi.org/10.1016/j.marpetgeo.2019.03.004.
- Xiao, H., Li, M.J., Yang, Z., et al., 2019b. The distribution patterns and geochemical implication of C<sub>19</sub>-C<sub>23</sub> tricyclic terpanes in source rocks and crude oils occurred in various depositional environment. Acta Geochem 48, 161–170. https://doi.org/10.19700/j.0379-1726.2019.02.006 (in Chinese with English abstract).
- Xiao, H., Wang, T.G., Li, M.J., et al., 2021. Organic geochemical heterogeneity of the Cretaceous Abu Gabra Formation and reassessment of oil sources in the Sufyan sub-basin, Sudan. Org. Geochem. 162, 104301. https://doi.org/10.1016/ j.orggeochem.2021.104301.

- Xiao, H., Wang, T.G., Li, M.J., et al., 2019c. Geochemical characteristics of Cretaceous Yogou Formation source rocks and oil-source correlation within a sequence stratigraphic framework in the Termit Basin, Niger. J. Petrol. Sci. Eng. 172, 362–372. https://doi.org/10.1016/j.petrol.2018.09.082.
- Xiao, H., Li, M.J., Nettersheim, B.J., 2024. Short chain tricyclic terpanes as organic proxies for paleo-depositional conditions. Chem. Geol. 652, 122023. https:// doi.org/10.1016/j.chemgeo.2024.122023.
- Yassin, M.A., Hariri, M.M., Abdullatif, O.M., et al., 2018. Sedimentologic and reservoir characteristics under a tectono-sequence stratigraphic framework: A case study from the Early Cretaceous, upper Abu Gabra sandstones, Sufyan Sub-basin, Muglad Basin, Sudan. J. Afr. Earth Sci. 142, 22–43. https://doi.org/10.1016/ j.jafrearsci.2018.02.015.
- You, B., Ni, Z.Y., Zeng, J.H., et al., 2020. Oil-charging history constrained by

- biomarkers of petroleum inclusions in the Dongying Depression. China. Mar. Petrol. Geol. 122, 104657. https://doi.org/10.1016/j.marpetgeo.2020.104657.
- Zhang, Z.H., Qin, L.M., Qiu, N.S., et al., 2010. Combination and superimposition of source kitchens and their effects on hydrocarbon accumulation in the hinterland of the Junggar Basin, west China. Pet. Sci. 7, 59—72. https://doi.org/10.1007/s12182-010-0007-y.
- Zumberge, J.E., 1987. Prediction of source rock characteristics based on terpane biomarkers in crude oils: A multivariate statistical approach. Geochim. Cosmochim. Acta 51, 1625–1637. https://doi.org/10.1016/0016-7037(87)90343-7.
- Zumberge, J.E., Harold, I., Stephen, B., et al., 2000. ABSTRACT: Biomarker Geochemistry of Lacustrine-sourced Crude Oils. A Worldwide Survey. https://doi.org/10.1306/a967525a-1738-11d7-8645000102c1865d.